RMxAC, **58**, 42–44 (2024)

THE EXTREMELY YOUNG PLANETARY NEBULA M 3-27

Francisco Ruiz-Escobedo[1], Miriam Peña[1], and Ana Valeria Beltrán-Sánchez[1]

RESUMEN

En esta memoria presentamos resultados parciales del análisis espectrofotométrico de la joven nebulosa planetaria M 3-27. Las líneas de H^+ tienen perfiles y velocidades radiales diferentes a las líneas de los demás iones, lo cual sugiere que son emitidas por la estrella central; debido a esto, la corrección por enrojecimiento se determinó utilizando las líneas de He^+. Encontramos la presencia de una zona interna de alta densidad electrónica (10^7 cm^{-3}) que dificulta el cálculo de la temperatura electrónica. Calculamos las abundancias iónicas relativas a He^+, que se escalaron para obtener las abundancias iónicas relativas a H^+, así como las abundancias totales.

ABSTRACT

In this proceeding we present partial results of the spectrophotometric analysis of the young planetary nebula M 3-27. The H^+ lines have different profiles and radial velocities than the lines of the other ions, suggesting that they are emitted from the central star. Therefore, the correction for reddening was determined using the He^+ lines. We find the presence of an internal zone with a high electron density (10^7 cm^{-3}), which complicates the calculation of the electron temperature. We calculated ionic abundances relative to He^+, which were then escalated to obtain ionic abundances relative to H^+, as well as total abundances.

Key Words: ISM: abundances — ISM: kinematics and dynamics — planetary nebulae: individual: M 3-27

1. INTRODUCTION

Planetary nebulae (PNe) represent one of the last evolutionary stages of low-intermediate initial mass stars ($\sim 1 - 8$ M$_\odot$). These objects are constituted by shells of gas expanding around a central star, which emits UV photons that ionize the gas. Emission lines of different ions, produced by various mechanisms, are detected in PNe spectra, such as collisionaly excited lines (CELs) and optical recombination lines (ORLs).

Physical conditions of PNe, electronic temperature (T_e) and electronic density (n_e), can be inferred from different CELs and ORLs ratios, e.g., n_e from [S II] $\lambda\lambda$6731/6716 and O II $\lambda\lambda$4649/4661, T_e from [O III] $\lambda\lambda(5007 + 4959)/4363$ and He I $\lambda\lambda$7281/6678. Once physical condition are determined, ionic abundances (X^{+i}/H^+) and total abundances of an element (X/H) are calculated.

M 3-27 is a young and compact PN, whose behaviour has been analysed since the late 1960s. Kohoutek (1968), Adams (1975), Ahern (1978) and Barker (1978) found that M 3-27 exhibits a density gradient, with an outer zone where $n_e \sim 10^3 - 10^4$ cm^{-3}, an inner zone where $n_e \geq 10^6$ cm^{-3}, and H I Balmer lines are affected by self-absorption. Wesson et al. (2005) estimated a $T_e = 13,000$ K and determined ionic and total abundances. Miranda et al. (1997) reported that Hα has different profile and velocity than CELs: Hα exhibits a P-Cygni profile, attributed to a strong stellar wind, and broad and extended wings up to 1500 km s^{-1}, attributed to Rayleigh-Raman photon scattering (Arrieta & Torres-Peimbert 2003).

In this proceeding, we present partial results of our analysis of M 3-27, complete results are presented and discussed in detail in the published paper Ruiz-Escobedo et al. (2024).

2. OBSERVATIONS

For this work, we analysed a set of optical spectra of M 3-27 obtained using Boller & Chivens and REOSC-Echelle spectrographs, which were attached to the 2.1-m telescope at Observatorio Astronómico Nacional San Pedro Mártir (OAN-SPM), Mexico, from 2004 to 2022. Boller & Chivens (B&Ch) spectra (2004 and 2021) provide a spectral resolution of $R = 685$ at 5000 Å. REOSC-Echelle spectra (2004, 2019, 2021 and 2022), provide spectral resolutions between $R \sim 16,000 - 18,000$ at 5000 Å. These spectra were reduced following the standard routines in IRAF[2] and were calibrated in wavelength and flux.

[1]Instituto de Astronomía, Universidad Nacional Autónoma de México, Apdo. Postal 70264, Ciudad Universitaria, 04510, Ciudad de México, México (fdruiz, miriam, avbeltran@astro.unam.mx).

[2]IRAF is distributed by the National Optical Observatory, which is operated by the Associated Universities for Research in Astronomy, Inc., under contract to the National Science Foundation.

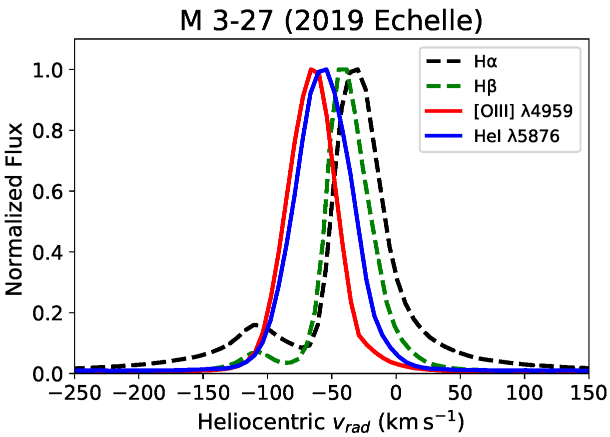

Fig. 1. Profiles and v_{rad} of important lines. (Reproduced from Figure 4 in Ruiz-Escobedo et al. (2024)).

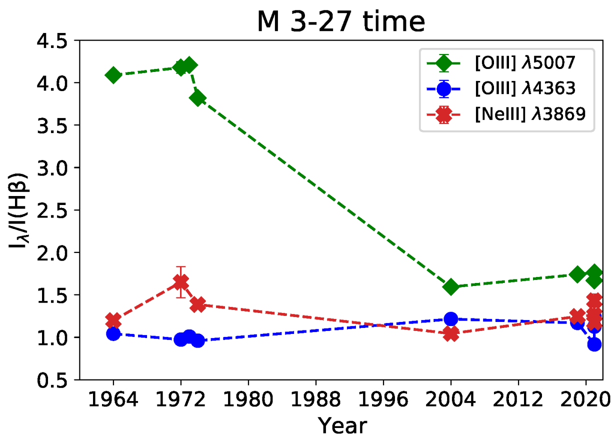

Fig. 2. Line evolution of important lines. (Reproduced from Figure 3 in Ruiz-Escobedo et al. (2024)).

3. ANALYSIS

3.1. *Line profiles*

We were able to analyse the line profiles from our REOSC-Echelle spectra due to their high-resolution. In Figure 1, we present the heliocentric radial velocities ($v_{\rm rad}$) of Hα, Hβ, He I λ5876, and [O III] λ4959 lines as observed in REOSC-Echelle 2019 spectrum. We found that He I λ5876 and [O III] λ4959 lines have a $v_{\rm rad} \sim -70$ km s^{-1} and show a single profile, however, Hα and Hβ lines exhibits a P-Cygni profile with two emission peaks, one blue at -84 km s^{-1} and another red at -7 km s^{-1}. Both H I lines also show an absorption that fits in velocity with He I and [O III] line profiles. Hα profile exhibits wide wings that extends up to 1,500 km s^{-1} attributed to Raman scattering. These characteristics were found in all the REOSC-Echelle spectra, indicating that H I lines are affected by stellar emission, which cannot be subtracted, whereas the lines of other ions are emitted by the nebula.

3.2. *Reddening correction*

Because of the stellar contribution to H I lines, the extinction correction of M 3-27 was performed using He I lines. For this purpose, we used the methodology proposed by Zamora et al. (2022) based on the observed fluxes and theoretical intensities of $\lambda\lambda$7281, 6678, 5875 and 4922 lines relative to λ6678, which serves as the reference wavelength ($f(\lambda_{\rm ref})$). These lines, which are unaffected by effects of $n_{\rm e}$, are plotted as points in the plane $\log(F_\lambda/F_\lambda^{\rm ref}) - \log(I_\lambda/I_\lambda^{\rm ref}) = f(\lambda) - f(\lambda_{\rm ref})$ and a linear regression is applied, the slope of the regression represents the value of c(Hβ). We obtained values of c(Hβ) ranging from 0.39 to 0.63 for OAN-SPM observations, which were then used to correct the line intensities for effects of reddening.

3.3. *Temporal evolution of line intensities*

In Figure 2, we present the temporal evolution of the intensities relative to Hβ of some important lines of M 3-27 in a period between 1968 to 2021. Data from the 1970s are taken from the previous studies in literature, while data from the 2000s are from OAN-SPM observations. The [O III] nebular line λ5007 shows a decrement in its intensity, from ~ 4 Hβ in the 1970s to ~ 1.7 Hβ in the 2000s. In contrast, [O III] auroral line λ4363 remaining at ~ 1 Hβ during all the period. A similar effect is also observed in the nebular and auroral lines of [O II], [N II] and [S II]. [Ne III] λ3869 does not show either important changes in its intensity, remaining at $\sim$ 1.5 Hβ.

This effect is attributed to an increase in the plasma $n_{\rm e}$, which suppresses the emission of nebular lines because these lines have lower critical densities ($n_{\rm crit}$) than the auroral lines. An increase in the plasma n_e throughout the period has been found a will be discussed in the next sections.

We also found a significant increase in Hα intensity, from ~ 4 Hβ to ~ 12 Hβ in 2021. This confirms that Hα emission is affected by stellar emission and suggests substantial changes in stellar emission over a short period of time.

3.4. *Physical conditions*

Physical conditions and abundances were calculated using PyNeb (Luridiana et al. 2015). From OAN-SPM data, we also found the presence of a density gradient in M 3-27, an outer zone where $n_{\rm e} \sim 10^3$ cm^{-3} and an inner zone where $n_{\rm e} = 10^7$ cm^{-3}; besides, most of the line diagnostic ratios used for $T_{\rm e}$ determination are showed more sensitive to $n_{\rm e}$, therefore, the estimation of a $T_{\rm e}$ becomes difficult.

TABLE 1

REPRESENTATIVE ABUNDANCES OF M 3-27

	Echelle 2019	B&Ch 2021
CELs		
O^+/H^+ ($\times 10^{-7}$) Neb.	$0.63^{+0.31}_{-0.24}$	—
O^+/H^+ ($\times 10^{-5}$) Aur.	—	$1.60^{+0.78}_{-0.49}$
O^{+2}/H^+ ($\times 10^{-4}$)	$1.68^{+0.31}_{-0.32}$	$1.86^{+0.28}_{-0.25}$
N^+/H^+ ($\times 10^{-6}$) Neb.	2.29 ± 0.31	$2.20^{+0.28}_{-0.26}$
ORLs		
O^{+2}/H^+ ($\times 10^{-4}$)	$5.50^{+0.50}_{-0.55}$	—
ADF(O^{+2})	$3.26^{+0.81}_{-0.61}$	—
12+log(O/H)	$8.22^{+0.07}_{-0.09}$	8.30 ± 0.06
log(N/O)	1.55::	-0.87 ± 0.17

:: Very uncertain value.

By an assuming a $n_e = 10^7$ cm^{-3}, a $T_e \sim 17,000$ K is determined from the [O III] $\lambda\lambda(5007+4959)/4363$ line ratio for REOSC-Echelle 2019 and B&Ch 2021 spectra. From REOSC-Echelle 2019 spectrum, n_e and T_e from ORLs were determined: $n_e \sim 10^4$ cm^{-3} from O II $\lambda\lambda 4661/4649$ and a $T_e = 8,000$ K from He I $\lambda\lambda 7281/6678$ (by using Zhang et al. 2005 formula).

3.5. *Ionic and total abundances*

For ionic abundances calculations, two n_e zones and a single T_e were assumed for CELs, while a single n_e and T_e zone were assumed for ORLs. Since H I lines are affected by stellar emission, we determined ionic abundances relative to He I $\lambda 5876$ line ($\frac{X^{+i}}{He^+}$) using the following formula:

$$\frac{X^{+i}}{He^+} = \frac{I_\lambda}{I_{HeI5876}} \times \frac{\epsilon_{HeI5876}}{\epsilon_\lambda} \quad (1)$$

Where $I_\lambda/I_{HeI5876}$ is the line intensity relative to He I $\lambda 5876$ and $\epsilon_{HeI5876}/\epsilon_\lambda$ is the ratio of He I and the line emissivities. These values were escalated to obtain the ionic abundances relative to H^+ by assuming that $He^+/H^+ = He/H = 0.11$, the mean He/H for Galactic disc PNe (Kingsburgh & Barlow 1994). Therefore, ionic abundances relative to H^+ were calculated as: $\frac{X^{+i}}{H^+}{}_{(He^+)} = 0.11 \times \frac{X^{+i}}{He^+}$. Abundance discrepancy factor, ADF(O^{+2}), was also calculated.

Total abundances were determined from the ionic abundances and corrected using ionization correction factors (ICFs) by Kingsburgh & Barlow (1994). Representative abundances are presented in Table 1.

4. DISCUSSION

We found that the inner n_e has changed from 10^6 cm^{-3}, in the 1970s, to 10^7 cm^{-3} in the 2000's. This increment suppresses the emission of nebular lines with low $n_{\rm crit}$. Additionally, we identified significant changes in Hα/Hβ intensity, which we attribute to important variations in central star emission.

Our results show that almost all O in M 3-27 is present in the form of O^{+2} and O^+ has a minimal contribution to O/H total abundance. We derived a sub-solar 12+log(O/H) value, ranging from 8.22 to 8.30, which is lower than the 8.60 value reported by Wesson et al. (2005). The O^+ abundance has implications on the determination of total abundances of other elements, such as N, due the construction of their ICFs. As is shown in Table 1, if O^+ abundance is determined using the nebular line [O II] $\lambda 3727$, which is suppressed by effects of n_e, the total N abundance will be overestimated and highly uncertain. However, this is no the case if O^+ abundance is determined from the auroral line [O II] $\lambda 7325$, in which case the N abundance behaves accordingly to values of disc PNe. Therefore, we adopted the total abundances derived from B&Ch data. We also derived a ADF(O^{+2}) = 3.26 lower than the value of 5.48 reported by Wesson et al. (2005).

M 3-27 is a challenging PN for its analysis, due to its high density and its important changes in short periods of time. Further observations and analysis of M 3-27 are needed.

Acknowledgements: This work has received financial support from grant UNAM-PAPIIT IN111423.

REFERENCES

Adams, T. F. 1975, ApJ, 202, 114
Ahern, F. J. 1978, ApJ, 223, 901
Arrieta, A., & Torres-Peimbert, S. 2003, ApJS, 147, 97
Barker, T. 1978, ApJ, 219, 914
Kingsburgh, R. L., & Barlow, M. J. 1994, MNRAS, 271, 257
Kohoutek, L. 1968, Bulletin of the Astronomical Institutes of Czechoslovakia, 19, 371
Luridiana, V., Morisset, C., & Shaw, R. A. 2015, A&A, 573, A42
Miranda, L. F., Vazquez, R., Torrelles, J. M., Eiroa, C., & Lopez, J. A. 1997, MNRAS, 288, 777
Ruiz-Escobedo, F., Peña, M., & Beltrán-Sánchez, A. V. 2024, MNRAS, 528, 4228
Wesson R., Liu, X.-W., & Barlow, M. J., 2005, MNRAS, 362, 424
Zamora, S., Díaz, A. I., Terlevich, E., & Fernández, V. 2022, MNRAS, 516, 749
Zhang, Y., Liu, X. W., Liu, Y., & Rubin, R. H. 2005, MNRAS, 358, 457